

# Ti-Doped LiAlH<sub>4</sub> for Hydrogen Storage: Synthesis, Catalyst Loading and Cycling Performance

Xiangfeng Liu,<sup>†</sup> Henrietta W. Langmi,<sup>†</sup> Shane D. Beattie,<sup>†</sup> Felix F. Azenwi,<sup>†</sup> G. Sean McGrady,<sup>\*,†</sup> and Craig M. Jensen<sup>‡</sup>

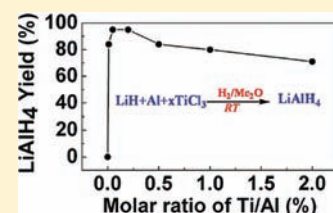
<sup>†</sup>Department of Chemistry, University of New Brunswick, P.O. Box 4400, Fredericton, New Brunswick E3B 5A3, Canada

<sup>‡</sup>Department of Chemistry, University of Hawaii at Manoa, Honolulu, Hawaii 96822-2275, United States

**S** Supporting Information

**ABSTRACT:** The direct synthesis of LiAlH<sub>4</sub> from commercially available LiH and Al powders in the presence of TiCl<sub>3</sub> and Me<sub>2</sub>O has been achieved for the first time. The effects of TiCl<sub>3</sub> loadings (Ti/Al = 0, 0.01, 0.05, 0.2, 0.5, 1.0 and 2.0%) and various other additives (TiCl<sub>3</sub>/Al<sub>2</sub>O<sub>3</sub>, metallic Ti, Nb<sub>2</sub>O<sub>5</sub>, and NbCl<sub>5</sub>) on the formation and stability of LiAlH<sub>4</sub> have been systematically investigated. The yield of LiAlH<sub>4</sub> initially increases, and then decreases, with increasing TiCl<sub>3</sub> loadings. LiH + Al → LiAlH<sub>4</sub> yields above 95% were obtained when the molar ratios of Ti/Al were 0.05 and 0.2%. In the presence of a very tiny amount of TiCl<sub>3</sub> (Ti/Al = 0.01%), LiAlH<sub>4</sub> is still generated, but the yield is lower. In the complete absence of TiCl<sub>3</sub>, LiAlH<sub>4</sub> does not form.

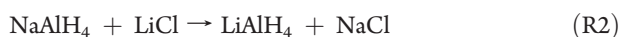
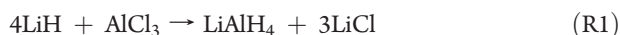
Addition of metallic Ti, Nb<sub>2</sub>O<sub>5</sub>, and NbCl<sub>5</sub> to commercial LiH and Al does not result in the formation of LiAlH<sub>4</sub>. Preliminary tests show that TiCl<sub>3</sub>-doped LiAlH<sub>4</sub> can be cycled, making it a suitable candidate for hydrogen storage.



## 1. INTRODUCTION

Safe and efficient hydrogen storage technology is one of the key technical barriers to the widespread commercialization of hydrogen-fueled vehicles.<sup>1–3</sup> Among the current hydrogen storage technologies, complex metal hydrides have received a lot of attention due to their high gravimetric H<sub>2</sub> capacity.<sup>4–6</sup> LiAlH<sub>4</sub> has a theoretical hydrogen storage capacity of 7.9 wt % and starts to desorb hydrogen close to room temperature in the presence of suitable catalysts, making it a potential hydrogen storage medium for future hydrogen-fueled vehicles.<sup>7,8</sup> However, the irreversibility of the dehydrogenation reactions of LiAlH<sub>4</sub> under practical conditions restricts its application as a suitable hydrogen storage medium. For example, rehydrogenation of LiH + Al to LiAlH<sub>4</sub> requires extremely high hydrogen pressures, in excess of 10 kbar.<sup>9</sup>

LiAlH<sub>4</sub> was first prepared through a reaction between LiH and AlCl<sub>3</sub> in ether solution (eq R1).<sup>10</sup> Later, a metathesis reaction was also successfully applied to synthesize LiAlH<sub>4</sub> (eq R2).<sup>11</sup> If LiAlH<sub>4</sub> is to be used as a hydrogen storage medium, neither of these routes will be suitable for practical regeneration of the dehydrogenated material (i.e., LiH + Al).



Direct synthesis of LiAlH<sub>4</sub> from its dehydrogenated products (LiH and Al) under moderate conditions is crucial if LiAlH<sub>4</sub> is to become a practical hydrogen storage material. In the 1960s, Ashby et al. reported the synthesis of LiAlH<sub>4</sub> from a mixture of LiH and activated Al in THF or diglyme solvent under 350 bar H<sub>2</sub> at 120 °C.<sup>12</sup> More recently, Wang et al. regenerated LiAlH<sub>4</sub>

from a mixture of LiH and Al through high-pressure and high-energy ball-milling in the presence of THF and catalyst.<sup>13,14</sup> In the latter study, the five-step physical and chemical pathway for rehydrogenation of LiAlH<sub>4</sub> required separation of catalyst in each cycle, and also the removal of THF by heating under vacuum over an extended period of time. In another study, Graetz et al. demonstrated a modified route to regenerate LiAlH<sub>4</sub> through an initial hydrogenation of Ti-catalyzed Al and LiH in THF to form the adduct LiAlH<sub>4</sub>·4THF, and subsequent desolvation to recover LiAlH<sub>4</sub>.<sup>15</sup> In this method, ethereal AlH<sub>3</sub> was first prepared through a reaction between LiAlH<sub>4</sub> and AlCl<sub>3</sub> in Et<sub>2</sub>O. With the addition of TiCl<sub>3</sub>, the ethereal solution of AlH<sub>3</sub> was dried and decomposed to obtain Ti-catalyzed Al under vacuum. The methods employing THF as the reaction medium all require a separate step for removal of the THF. It usually takes 4–6 h to remove THF completely at 60 °C under reduced pressure. Besides the efficiency and cost of these methods, it is also not easy to avoid the decomposition of Ti-doped LiAlH<sub>4</sub> during THF removal. Our group has reported a much simpler and energy-efficient single-stage regeneration procedure for Ti-doped LiAlH<sub>4</sub>.<sup>16</sup> In this method, a mixture of LiH and Al from the decomposition of TiCl<sub>3</sub>-catalyzed LiAlH<sub>4</sub> was rehydrogenated to form LiAlH<sub>4</sub> in the presence of volatile Me<sub>2</sub>O at room temperature. Dry Ti-doped LiAlH<sub>4</sub> powder was obtained directly after a cautious release of H<sub>2</sub> and excess Me<sub>2</sub>O. The use of Me<sub>2</sub>O not only delivers a high yield of LiAlH<sub>4</sub> but also avoids the time-consuming drying process.

In the work reported here, we have eliminated the initial dehydrogenation process of Ti-doped LiAlH<sub>4</sub> and directly synthesized the

Received: May 30, 2011

Published: August 24, 2011

doped material directly from commercially available LiH and Al powders, in the presence of a  $\text{TiCl}_3$ -derived catalyst and  $\text{Me}_2\text{O}$ . The effects of  $\text{TiCl}_3$  loadings ( $\text{Ti}/\text{Al} = 0, 0.01, 0.05, 0.2, 0.5, 1.0$ , and  $2.0$  mol %) and of other catalysts ( $\text{TiCl}_3/\text{Al}_2\text{O}_3$ , metallic Ti,  $\text{Nb}_2\text{O}_5$ , and  $\text{NbCl}_5$ ) on the formation of  $\text{LiAlH}_4$  have been systematically investigated. In addition, a preliminary study of the cycling performance of Ti-doped  $\text{LiAlH}_4$  and of  $\text{Ti}/\text{Al}_2\text{O}_3$ -doped  $\text{LiAlH}_4$  is presented.

## 2. EXPERIMENTAL METHODS

LiH (Aldrich, 95%), Al powder (Alfa Aesar,  $\sim 325$  mesh, 99.97%),  $\text{TiCl}_3$  (Aldrich, 99.999%), Ti (Aldrich,  $\sim 325$  mesh, 99.98%),  $\text{NbCl}_5$  (Aldrich, 99.9%),  $\text{Nb}_2\text{O}_5$  (Aldrich,  $\sim 325$  mesh, 99.9%), and  $\text{Al}_2\text{O}_3$  (BDH, type 60/E) were used as received. All materials and samples were handled in a nitrogen-filled glovebox. LiH/Al/catalyst (catalyst = 0.2 mol % Ti,  $\text{NbCl}_5$  or 0.1 mol %  $\text{Nb}_2\text{O}_5$ ) and LiH/Al/ $\text{TiCl}_3$  with various concentrations of  $\text{TiCl}_3$  (molar ratio of  $\text{Ti}/\text{Al} = 0, 0.01, 0.05, 0.2, 0.5, 1.0$ , and  $2.0\%$ ) were each mixed by ball-milling. In a typical experiment, a 5 g mixture of the powders was loaded in a 250 mL stainless steel milling vessel containing five stainless steel balls (about 162 g). The powder mixtures were mechanically milled at room temperature in a nitrogen atmosphere at a rotational speed of 300 rpm for 12 h using a Retsch PM 100 planetary ball-mill. After every 15 min of milling, there was a 30 s pause, and the rotation was automatically reversed.  $\text{Ti}/\text{Al}_2\text{O}_3$  catalyst was prepared by milling  $\text{TiCl}_3$  and  $\text{Al}_2\text{O}_3$  in a 1:4 mol ratio. Activation of the catalyst was carried out under an initial hydrogen pressure of 100 bar. The supported catalyst was heated to  $200^\circ\text{C}$  at a ramping rate of  $2^\circ\text{C min}^{-1}$ , and held at that temperature for 12 h using a PCTPro-2000 Sieverts-type instrument manufactured by HyEnergy LLC. The LiH/Al/ $\text{TiCl}_3/\text{Al}_2\text{O}_3$  (0.05 mol %  $\text{TiCl}_3$ ) mixture was recovered from the PCT vessel and ball-milled again.

Hydrogenation reactions in  $\text{Me}_2\text{O}$  (Air Liquide Canada Inc., chemically pure) were carried out in a 500 mL stainless steel stirred reactor (Parr Instruments). In a typical procedure, the reactor was loaded in a glovebox with 650 mg of the ball-milled LiH/Al/catalyst mixture. The reactor was sealed, removed from the glovebox, and connected to a  $\text{Me}_2\text{O}$  cylinder. Approximately 55 g of  $\text{Me}_2\text{O}$  was then transferred to the reactor. Next,  $\text{H}_2$  gas (100 bar) was added to the reactor. After 24 h of stirring at ambient temperature the reaction was stopped, and  $\text{H}_2$  and  $\text{Me}_2\text{O}$  were vented immediately.

Powder X-ray diffraction (XRD) was performed on a Rigaku MiniFlex II diffractometer with a  $\text{Cu K}\alpha$  radiation source. Samples for XRD analysis were mounted on a PVC plastic disk and covered with parafilm to protect the material from contact with air or moisture during the experiments. The parafilm resulted in two diffraction peaks ( $2\theta = 21.6$  and  $24^\circ$ ). Thermogravimetric analysis was performed on a TGA Q50 series thermogravimetric analyzer. In a typical procedure, approximately 8 mg of sample was loaded in an Al crucible in a nitrogen-filled glovebox. The sample was heated to  $300^\circ\text{C}$  at a ramping rate of  $2^\circ\text{C/min}$  under a  $\text{N}_2$  flow rate of 120 mL/min. Decomposition kinetics plots were obtained using a commercial PCTPro-2000 Sieverts-type instrument produced by HyEnergy LLC. In a typical experiment, approximately 350 mg of sample was loaded into a sample holder in a nitrogen-filled glovebox. The sample holder was then attached to the PCT instrument without exposing the sample to air. The sample was heated at a ramping rate of  $2^\circ\text{C/min}$  to  $250^\circ\text{C}$  and then held at this temperature for 30 min.

In addition, the morphology and elemental analysis of the samples were studied by transmission electron microscopy (JEOL 2011 Scanning TEM).

## 3. RESULTS AND DISCUSSION

### 3.1. Effect of $\text{TiCl}_3$ Loadings on the Formation and Stability of $\text{LiAlH}_4$ .

Previously, we reported the regeneration of

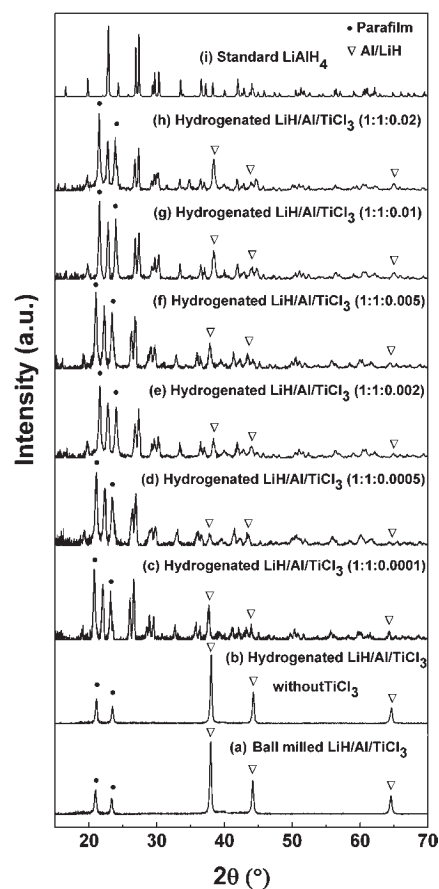


**Figure 1.** XRD patterns of ball-milled LiH/Al/ $\text{TiCl}_3$  and hydrogenated samples with various  $\text{TiCl}_3$  loadings: (a) ball-milled LiH/Al/ $\text{TiCl}_3$  (1:1:0.002); (b) hydrogenated LiH/Al/ $\text{TiCl}_3$  (1:1:0) without  $\text{TiCl}_3$ ; (c) hydrogenated LiH/Al/ $\text{TiCl}_3$  (1:1:0.0001); (d) hydrogenated LiH/Al/ $\text{TiCl}_3$  (1:1:0.0005); (e) hydrogenated LiH/Al/ $\text{TiCl}_3$  (1:1:0.002); (f) hydrogenated LiH/Al/ $\text{TiCl}_3$  (1:1:0.005); (g) hydrogenated LiH/Al/ $\text{TiCl}_3$  (1:1:0.01); (h) hydrogenated LiH/Al/ $\text{TiCl}_3$  (1:1:0.02); (i) standard  $\text{LiAlH}_4$  from ICDD.  $\text{LiAlH}_4$  formed after the hydrogenation of ball-milled LiH/Al/ $\text{TiCl}_3$ , but no  $\text{LiAlH}_4$  formed without the addition of  $\text{TiCl}_3$ .

Ti-doped  $\text{LiAlH}_4$  in  $\text{Me}_2\text{O}$  at room temperature.<sup>16</sup> In this earlier study,  $\text{LiAlH}_4$  was first doped with  $\text{TiCl}_3$  and then decomposed to LiH and Al, followed by rehydrogenation in  $\text{Me}_2\text{O}$ . In the subsequent work reported here, we have avoided this rehydrogenation approach. Instead, commercially available LiH and Al (1:1) were directly doped using different amounts of  $\text{TiCl}_3$  (molar ratio of  $\text{Ti}/\text{Al} = 0, 0.01, 0.05, 0.2, 0.5, 1.0$ , and  $2.0\%$ ) by ball-milling and then hydrogenated at room temperature in  $\text{Me}_2\text{O}$ . It is notable that much lower amounts of  $\text{TiCl}_3$  dopant are reported here. Figure 1 shows XRD patterns for ball-milled LiH/Al/ $\text{TiCl}_3$  (1:1:0.002) and the hydrogenated samples with various  $\text{TiCl}_3$  loadings. It is evident that these Ti-doped LiH/Al samples have been directly hydrogenated to  $\text{LiAlH}_4$ . The relative intensity of unreacted LiH/Al peaks decreases with decreasing amounts of  $\text{TiCl}_3$  down to  $\text{Ti}/\text{Al} = 0.2\%$ , indicating that lower  $\text{TiCl}_3$  loading favors the formation of  $\text{LiAlH}_4$  and increases its stability, in accordance with the catalyst activating both hydrogen uptake and release. However, when the  $\text{TiCl}_3$  content was further lowered to 0.01% ( $\text{Ti}/\text{Al}$ ),  $\text{LiAlH}_4$  formed but the intensity of unreacted LiH/Al peaks increased slightly. The yield of  $\text{LiAlH}_4$  as

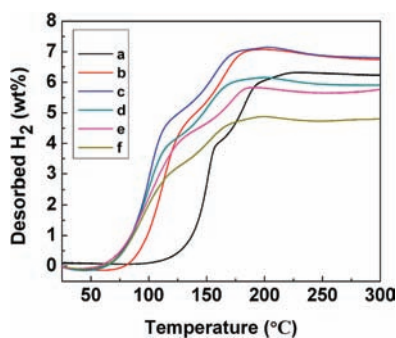


**Figure 2.** Temperature-programmed desorption (TPD) curves measured by TGA: (a) hydrogenated LiH/Al/TiCl<sub>3</sub> (1:1:0.0001); (b) hydrogenated LiH/Al/TiCl<sub>3</sub> (1:1:0.0005); (c) hydrogenated LiH/Al/TiCl<sub>3</sub> (1:1:0.002); (d) hydrogenated LiH/Al/TiCl<sub>3</sub> (1:1:0.005); (e) hydrogenated LiH/Al/TiCl<sub>3</sub> (1:1:0.01); (f) hydrogenated LiH/Al/TiCl<sub>3</sub> (1:1:0.02).

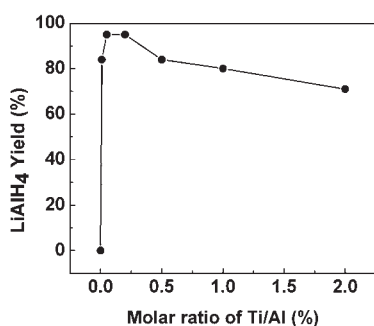


**Figure 3.** Dependence of LiAlH<sub>4</sub> yield on the loading of TiCl<sub>3</sub> (molar ratio of Ti/Al).

a function of TiCl<sub>3</sub> loadings is discussed below. Undoped LiH/Al (Figure 1b) could not be hydrogenated to LiAlH<sub>4</sub>, indicating that a very small but nonzero amount of TiCl<sub>3</sub> is necessary for the formation of LiAlH<sub>4</sub>. It should be pointed out that the diffraction peaks of LiH are difficult to discern (Figure 1a) on account of the low atomic numbers of the elements, because LiH becomes amorphous after ball-milling, and/or because its peaks overlap with those of Al.<sup>13,14</sup>

Figure 2 shows temperature-programmed desorption (TPD) curves of hydrogenated samples with various TiCl<sub>3</sub> loadings. The TPD curves were derived from TGA data. The maximum amounts of desorbed H<sub>2</sub> for LiH/Al/*x*TiCl<sub>3</sub> (*x* = 0.0001, 0.0005, 0.002, 0.005, 0.01, and 0.02) were 6.3, 7.1, 7.1, 6.2, 5.8, and 4.9 wt %, respectively. Considering the purity of LiH (95%) and the maximum hydrogen content of LiAlH<sub>4</sub> (7.5 wt %, 95% purity), the yields of LiAlH<sub>4</sub> were calculated to be 84, 95, 95, 84, 80, and 71%, respectively. The dependence of the LiAlH<sub>4</sub> yield on the loading of TiCl<sub>3</sub> is presented in Figure 3. The yield of LiAlH<sub>4</sub> tends to increase with decreasing TiCl<sub>3</sub> loading down to *x* = 0.002, and then decreases as *x* drops to 0.0001, in agreement with XRD analysis. The results also indicate that the TiCl<sub>3</sub>-derived catalyst acts in both directions: it promotes the conversion of LiH/Al to LiAlH<sub>4</sub>, and it activates the decomposition of LiAlH<sub>4</sub> to Li<sub>3</sub>AlH<sub>6</sub> or LiH/Al. Under the current reaction conditions (room temperature and 100 bar H<sub>2</sub>), a low Ti/Al proportion of 0.05–0.2% provides the optimum balance between conversion to LiAlH<sub>4</sub> and stability of LiAlH<sub>4</sub>, resulting in a high yield. However, LiAlH<sub>4</sub> did not form at all when LiH/Al was ball-milled

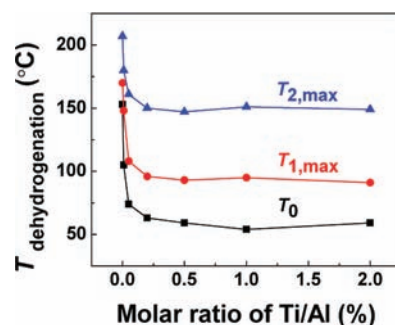


**Figure 4.** Dependence of dehydrogenation temperature on the loading of TiCl<sub>3</sub> (molar ratio of Ti/Al).  $T_0$ ,  $T_{1,max}$  and  $T_{2,max}$  represent the onset dehydrogenation temperature, the dehydrogenation temperature at the maximum desorption rate during the first-stage dehydrogenation, and the dehydrogenation temperature at the maximum desorption rate during the second-stage dehydrogenation, respectively.

without TiCl<sub>3</sub>, indicating the crucial role of tiny amounts of Ti in the formation of LiAlH<sub>4</sub>. TiCl<sub>3</sub> shows a high catalytic efficiency in this system, and the loadings of TiCl<sub>3</sub> used in this study were much lower than those used in the previously reported THF-based synthesis of LiAlH<sub>4</sub>,<sup>15</sup> or of the widely studied NaAlH<sub>4</sub> system,<sup>17</sup> where 2 mol % Ti is typically used. In this study, high TiCl<sub>3</sub> loadings (Ti/Al > 0.5%) result in a significant decrease in the yield, because LiAlH<sub>4</sub> is less thermodynamically stable than its Na congener, and higher TiCl<sub>3</sub> loadings promote decomposition of LiAlH<sub>4</sub>. A two-stage decomposition of Ti-doped LiAlH<sub>4</sub> can be clearly observed in Figure 2, in agreement with previous studies.<sup>7,18</sup>

Figure 4 shows the dependence of dehydrogenation temperature on the loading of TiCl<sub>3</sub> (molar ratio of Ti/Al).  $T_0$  represents the onset dehydrogenation temperature,  $T_{1,max}$  represents the dehydrogenation temperature at the maximum desorption rate on the first stage of dehydrogenation, and  $T_{2,max}$  represents the dehydrogenation temperature at the maximum desorption rate on the second stage of dehydrogenation.  $T_0$ ,  $T_{1,max}$  and  $T_{2,max}$  each show a significant decrease with increasing TiCl<sub>3</sub> loading (Ti/Al < 0.2%). When Ti/Al is above 0.2%, the dehydrogenation temperature changes slightly, indicating that a small amount of TiCl<sub>3</sub> greatly decreases the dehydrogenation temperature of LiAlH<sub>4</sub> and an excess of TiCl<sub>3</sub> might aggregate to form some “Ti-rich” areas (clusters) during the venting of H<sub>2</sub> and Me<sub>2</sub>O. The activity of the Ti catalyst will be degraded by the formation of Ti clusters.

To investigate the formation of “Ti-rich” clusters, a TEM study was performed on a rehydrogenated LiH/Al/TiCl<sub>3</sub> (1:1:0.005) sample. Figure S1 shows an EDAX pattern measured for this sample, with the corresponding TEM image inset. This particle was chosen for its high Ti content. According to energy-dispersive X-ray (EDX) analysis, the composition of this particle is ~96% Ti and 4% Al, strongly suggesting that the Ti aggregates during cycling. This aggregation may explain the falloff in cycling performance. After each de-/rehydrogenation cycle, the Ti catalyst agglomerates into large particles with low surface area, that are not necessarily in contact with the majority of the LiAlH<sub>4</sub>/LiH/Al sample.

**3.2. Dehydrogenation Kinetics of Synthesized Ti-Doped LiAlH<sub>4</sub>.** The decomposition kinetics of Ti-doped LiAlH<sub>4</sub> was investigated by means of a Sieverts-type apparatus. As shown in Figure S2, as-received LiAlH<sub>4</sub> can release 7.5 wt % H. The

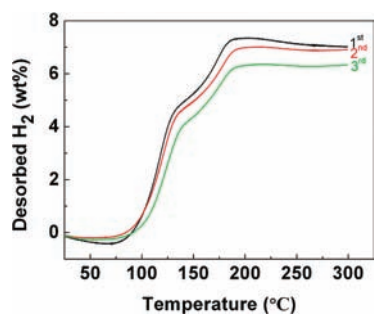


**Figure 5.** Cycling performance of  $\text{TiCl}_3$ -catalyzed  $\text{LiAlH}_4$  as measured by TGA. The amount of  $\text{H}_2$  desorbed in the first, second, and third cycles is 7.3, 7.0, and 6.4 wt %, respectively.

desorbed hydrogen contents for the hydrogenated  $\text{LiH}/\text{Al}/x\text{TiCl}_3$  ( $x = 0.0005$  and  $0.005$ ) are 7.1 and 6.1 wt %, respectively, in excellent agreement with the TGA data reported in Figure 2. From the slope of the curves, the two-stage decomposition of as-received and synthesized Ti-doped  $\text{LiAlH}_4$  can be clearly observed. Compared to as-received  $\text{LiAlH}_4$ , the onset decomposition temperature for Ti-doped  $\text{LiAlH}_4$  is significantly lowered, to around  $80^\circ\text{C}$ . The onset temperature for hydrogenated  $\text{LiH}/\text{Al}/\text{TiCl}_3$  (1:1:0.005) was lower than that for hydrogenated  $\text{LiH}/\text{Al}/\text{TiCl}_3$  (1:1:0.0005), demonstrating that the dehydrogenation temperature of  $\text{TiCl}_3$ -catalyzed  $\text{LiAlH}_4$  decreases with increasing  $\text{TiCl}_3$  concentration. However, it should be noted that the dehydrogenation temperature did not significantly change when a certain loading level of  $\text{TiCl}_3$  ( $\text{Ti}/\text{Al} > 0.2\%$ ) was reached (as discussed above).

**3.3. Hydrogenation–Dehydrogenation Cycling Performance of Ti-Doped  $\text{LiAlH}_4$ .** About 1 g of Ti-doped  $\text{LiAlH}_4$  that was prepared from the hydrogenation of  $\text{LiH}/\text{Al}/\text{TiCl}_3$  (1:1:0.0005) was first dehydrogenated at  $120^\circ\text{C}$  under a dynamic vacuum. Ball-milling was performed on the sample before each successive rehydrogenation in order to ensure proper dispersion of the catalyst, which may have agglomerated as a result of the dehydrogenation procedure (as discussed above). The dehydrogenated sample was rehydrogenated under the same conditions as the initial synthesis of  $\text{LiAlH}_4$ . The hydrogen capacity of the rehydrogenated sample was measured by TGA. The remaining sample was decomposed at  $120^\circ\text{C}$  under dynamic vacuum for a second and third time and rehydrogenated under the same conditions. Figure 5 reports the amount of desorbed  $\text{H}_2$  obtained from these three cycles: 7.3, 7.0, and 6.4 wt %, respectively, indicating the potential of  $\text{TiCl}_3$ -doped  $\text{LiAlH}_4$  as a rechargeable hydrogen storage system. However, it was noted that the temperature for hydrogen release increased slightly with successive cycles; this may be attributed to gradual loss in catalytic activity or degradation of the active catalyst species, which is present only in very low amounts.

**3.4. Effects of  $\text{Al}_2\text{O}_3$ -Supported Ti on the Hydrogen Storage Performance of  $\text{LiAlH}_4$ .** In an attempt to investigate further the cycling performance of  $\text{TiCl}_3$ -doped  $\text{LiAlH}_4$ ,  $\text{TiCl}_3$  was deposited on an  $\text{Al}_2\text{O}_3$  support. It was anticipated that this support may help to maintain a uniform distribution of the catalyst upon cycling, eliminating the need for ball-milling before successive rehydrogenation procedures, and improving the cyclic performance. The supported catalyst  $\text{Ti}/\text{Al}_2\text{O}_3$  was prepared in a 1:4 mol ratio and activated with hydrogen at  $200^\circ\text{C}$ . The reactant mixture ( $\text{LiH}$  and  $\text{Al}$ ) was then doped with 0.05 mol % of this

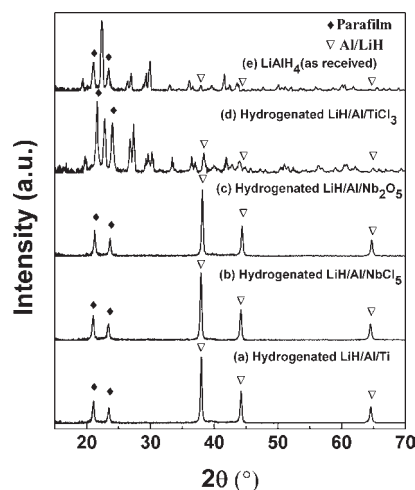


**Figure 6.** XRD patterns for hydrogenated samples with different additives (additive/ $\text{Al} = 0.2\%$ ): (a) hydrogenated  $\text{LiH}/\text{Al}/\text{Ti}$ ; (b) hydrogenated  $\text{LiH}/\text{Al}/\text{NbCl}_5$ ; (c) hydrogenated  $\text{LiH}/\text{Al}/\text{Nb}_2\text{O}_5$ ; (d) hydrogenated  $\text{LiH}/\text{Al}/\text{TiCl}_3$ ; (e) as-received  $\text{LiAlH}_4$ . No  $\text{LiAlH}_4$  formed when metallic  $\text{Ti}$ ,  $\text{NbCl}_5$ , or  $\text{Nb}_2\text{O}_5$  was added in place of  $\text{TiCl}_3$ .

supported  $\text{Ti}$  and hydrogenated in  $\text{Me}_2\text{O}$ . This amount of catalyst was chosen because it gave the best performance in terms of yield and stability when neat  $\text{TiCl}_3$  was used as a dopant (Section 3.1). A hydrogen desorption capacity of 5.9 wt % was obtained for the hydrogenated  $\text{LiH}/\text{Al}/\text{TiCl}_3/\text{Al}_2\text{O}_3$  product (Figure S3). After dehydrogenation and subsequent rehydrogenation, the hydrogen capacity dropped to 4.0 wt % in the second cycle. The supported  $\text{Ti}/\text{Al}_2\text{O}_3$  catalyst lowered the hydrogen desorption temperature, with release commencing at ca.  $125^\circ\text{C}$  as opposed to  $180^\circ\text{C}$  for the undoped material. Hydrogen desorption during the second cycle started at a higher temperature ( $140^\circ\text{C}$ ) than for the first cycle ( $125^\circ\text{C}$ ). It is possible that the  $\text{Ti}$  catalyst became detached from the support upon cycling and did not remain properly dispersed, thereby reducing its effectiveness. Hence, the cycling performance of the  $\text{Ti}/\text{Al}_2\text{O}_3$ -catalyzed material was found to be inferior to that of the straightforward Ti-doped  $\text{LiAlH}_4$ . Given the additional weight of the  $\text{Al}_2\text{O}_3$  support, we conclude that there is no advantage to using a  $\text{Ti}$  catalyst in this form for the hydrogen cycling of  $\text{LiAlH}_4$ .

**3.5. Effects of Metallic  $\text{Ti}$ ,  $\text{Nb}_2\text{O}_5$ , and  $\text{NbCl}_5$  Additives on the Formation of  $\text{LiAlH}_4$ .** The effects of other additives (metallic  $\text{Ti}$ ,  $\text{Nb}_2\text{O}_5$ , and  $\text{NbCl}_5$ ) on the formation of  $\text{LiAlH}_4$  from commercial  $\text{LiH}$  and  $\text{Al}$  were also investigated. However, under the experimental conditions described in Section 2, none of these resulted in the formation of  $\text{LiAlH}_4$ , as reported in Figure 6.

Extensive studies have been performed on the catalyzed  $\text{NaAlH}_4$  system.<sup>18–23</sup> However, the details of the role of titanium halide catalysts in the improved reversibility of  $\text{NaAlH}_4$  are still unclear. An initial reduction reaction was suggested, and X-ray absorption spectroscopy confirmed that reduction of the original  $\text{TiCl}_3$  in fact occurs, with  $\text{Ti(III)}$  being reduced to  $\text{Ti(0)}$  when  $\text{NaAlH}_4$  was ball-milled with  $\text{TiCl}_3$ , and remaining in this oxidation state during subsequent desorption and absorption of hydrogen.<sup>21</sup> The structure formed after ball-milling was close to that of metallic  $\text{Ti}$  but in a more distorted state. The formation of  $\text{LiCl}$  and the reduction of  $\text{Ti(IV)}$  were observed when  $\text{LiAlH}_4$  was ball-milled with  $\text{TiCl}_4$  in an early study.<sup>24</sup> As to the catalytic

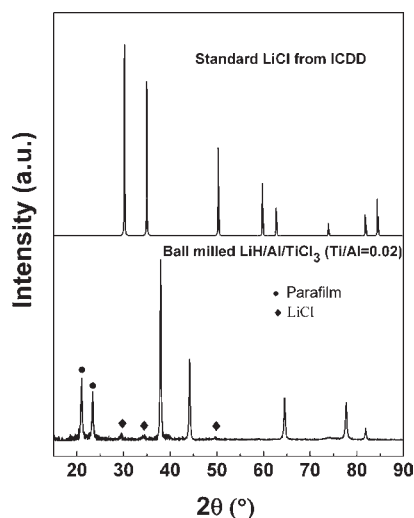


**Figure 7.** XRD patterns of standard LiCl from ICDD and ball-milled LiH/Al/TiCl<sub>3</sub> (1:1:0.02). LiCl was observed in the ball-milled mixture of LiH/Al/TiCl<sub>3</sub>.

mechanism of our LiH/Al/TiCl<sub>3</sub> system, there might be some differences owing to the utilization of Me<sub>2</sub>O. Interestingly, LiCl also formed after the mixture of LiH/Al/TiCl<sub>3</sub> was ball-milled (see Figure 7), and Ti(3+) might have a similar reduction in oxidation state during the ball-milling process. A detailed study of the catalytic mechanism of the conversion of LiH/Al to LiAlH<sub>4</sub> is still in progress.

#### 4. CONCLUSIONS

In summary, we have succeeded in directly preparing Ti-doped LiAlH<sub>4</sub> from commercially available LiH and Al through the use of a TiCl<sub>3</sub> additive and Me<sub>2</sub>O solvent. The yield of LiAlH<sub>4</sub> first increased and then decreased with increasing TiCl<sub>3</sub> content. A low percentage of TiCl<sub>3</sub> (TiCl<sub>3</sub>/Al = 0.05–0.2%) provides the optimum balance between the formation and stability of LiAlH<sub>4</sub>, resulting in a high yield. However, LiAlH<sub>4</sub> did not form at all without the addition of TiCl<sub>3</sub>. Furthermore, metallic Ti, Nb<sub>2</sub>O<sub>5</sub>, and NbCl<sub>5</sub> did not show any catalytic activity, and LiAlH<sub>4</sub> was not generated in the hydrogenation reactions. The hydrogenated TiCl<sub>3</sub>-doped samples released more than 7 wt % hydrogen, with an onset dehydrogenation temperature of 80 °C. The dehydrogenated material could be cycled, with the material retaining about 6.4 wt % H capacity after three cycles. Al<sub>2</sub>O<sub>3</sub>-supported Ti showed some cycling ability but was deemed inferior to straightforward TiCl<sub>3</sub>-doped LiAlH<sub>4</sub>, which shows significant promise as a reversible, high-capacity hydrogen storage material.

#### ■ ASSOCIATED CONTENT

**S Supporting Information.** EDAX spectrum with TEM image inset, dehydrogenation kinetics curves measured by a Sieverts-type apparatus, and cycling performance of TiCl<sub>3</sub>/Al<sub>2</sub>O<sub>3</sub>-catalyzed LiAlH<sub>4</sub>. This material is available free of charge via the Internet at <http://pubs.acs.org>.

#### ■ AUTHOR INFORMATION

**Corresponding Author**  
smcgrady@unb.ca

#### ■ ACKNOWLEDGMENT

We are grateful to NSERC of Canada, the Canadian Foundation for Innovation, the U.S. Department of Energy, and HSM Systems Inc. for support of this work.

#### ■ REFERENCES

- Schlapbach, L.; Züttel, A. *Nature* **2001**, *414*, 353.
- Ritter, J. A.; Ebner, A. D.; Wang, J.; Zidan, R. *Mater. Today* **2003**, *6*, 18.
- Mandal, T. K.; Gregory, D. H. *Annu. Rep. Prog. Chem. Sect. A* **2009**, *105*, 21.
- Graetz, J. *Chem. Soc. Rev.* **2009**, *38*, 73.
- Chen, P.; Zhu, M. *Mater. Today* **2008**, *12*, 36.
- Orimo, S.; Nakamori, Y.; Eliseo, J. R.; Züttel, A.; Jensen, C. M. *Chem. Rev.* **2007**, *107*, 4111.
- Andreasen, A. J. *Alloys Compd.* **2006**, *419*, 40.
- Chen, J.; Kuriyama, N.; Xu, Q.; Takeshita, T.; Sakai, T. *J. Phys. Chem. B* **2001**, *105*, 11214.
- Varin, R. A.; Czujko, T.; Wronski, Z. S. *Nanomaterials for Solid State Hydrogen Storage*; Springer: Berlin, 2009.
- Finholt, A. E.; Bond, A. C.; Schlesinger, H. I. *J. Am. Chem. Soc.* **1947**, *69*, 1199.
- Bragdon, R. W.; Del Giudice, F. P. U.S. Patent 3,162,508, 1964.
- Ashby, E. C.; Brendel, G. J.; Redman, H. E. *Inorg. Chem.* **1963**, *2*, 499.
- Wang, J.; Ebner, A. D.; Ritter, J. A. *J. Am. Chem. Soc.* **2006**, *128*, 5949.
- Wang, J.; Ebner, A. D.; Ritter, J. A. *J. Phys. Chem. C* **2007**, *111*, 14917.
- Graetz, J.; Wegrzyn, J.; Reilly, J. J. *J. Am. Chem. Soc.* **2008**, *130*, 17790.
- Liu, X. F.; McGrady, G. S.; Langmi, H. W.; Jensen, C. M. *J. Am. Chem. Soc.* **2009**, *131*, 5032.
- Bogdanović, B.; Schwickardi, M. *J. Alloys Compd.* **1997**, *253*, 1.
- Langmi, H. W.; McGrady, G. S.; Liu, X.; Jensen, C. M. *J. Phys. Chem. C* **2010**, *114*, 10666.
- Wang, P.; Jensen, C. M. *J. Phys. Chem. B* **2004**, *108*, 15827.
- Bogdanović, B.; Brand, R. A.; Marjanović, A.; Schwickardi, M.; Tölle, J. *J. Alloys Compd.* **2000**, *302*, 36.
- Leon, A.; Kircher, O.; Rothe, J.; Fichtner, M. *J. Phys. Chem. B* **2004**, *108*, 16372.
- Brinks, H. W.; Jensen, C. M.; Srinivasan, S. S.; Hauback, B. C.; Blanchard, D.; Murphy, K. *J. Alloys Compd.* **2004**, *376*, 215.
- Kuba, M. T.; Eaton, S. S.; Morales, C.; Jensen, C. M. *J. Mater. Res.* **2005**, *20*, 3265.
- Balema, V. P.; Dennis, K. W.; Pecharsky, V. K. *Chem. Commun.* **2000**, *17*, 1665.